Ab initio study of atomic structure and Schottky barrier height at the GaAs/$Ni_{0.5}Pt_{0.5}Ge$ interface

Manish K. Niranjan, Leonard Kleinman, and Alexander A. Demkov*
Department of Physics, The University of Texas at Austin, Austin, Texas 78712, USA
(Received 31 August 2007; revised manuscript received 19 December 2007; published 16 April 2008)

We report a study of the atomic and electronic structures of GaAs(001)/NiPtGe(001) interfaces. By using density functional theory, we study the dependence of the Schottky barrier on the interface stoichiometry. The calculated *p*-type Schottky barrier heights vary by as much as 0.18 eV around the average value of 0.5 eV, which corresponds to a strongly pinned interface. We relate the As-Ge bonds at the interface with a strong Fermi level pinning.

DOI: 10.1103/PhysRevB.77.155316 PACS number(s): 71.55.Ak, 71.20.Be, 71.20.Nr, 73.61.At

I. INTRODUCTION

Reaching the fundamental materials limits of Si in complementary metal-oxide-semiconductor (CMOS) technology has led to intense research into alternative channel materials. III-V compound semiconductors, such as GaAs and InSb, have generated significant attention as potential candidates for a channel material in future CMOS-type devices, thanks to their high carrier mobility.[1–3] Compound semiconductors are also attractive for applications in which silicon cannot be used, such as optoelectronics, high-power devices, high frequency devices, and high temperature devices. However, despite many advantages, the development of alternative channel material devices is very challenging due to materials complexity. There are a number of issues that must be addressed before this new strategy can be implemented in CMOS manufacturing. One such issue is the contact resistance at the metal-semiconductor interface.[4] To fully exploit the transport properties of GaAs and other compound semiconductors, a low resistance contact technology will have to be developed, which is similar to that based on metal silicides, and used in Si CMOS.[5] Metal germanides show promise in making low resistance contacts for both III-V and Ge or $Si_{1-x}Ge_x$ based metal-oxide-semiconductor field effect transistors. The process is self-aligned and relies on a solid phase reaction of Ge and metals.[6–12] NiGe and possibly PtGe appear to be the most promising due to low formation temperature and low resistivity.[6–8] Interestingly, the binary Ni-Ge alloy system has been used to make contacts in non-CMOS GaAs devices.

The two main factors that determine the contact resistance in the device are the Schottky barrier height (SBH) at the metal/semiconductor interface and the doping concentration of impurities in the semiconductor.[13,14] The former is of fundamental interest as an intrinsic property of the system. *Ab initio* calculations provide the Schottky barrier estimate along with fundamental understanding of the interfacial atomic and electronic structure, which ultimately determine the barrier. GaAs has a complicated surface chemistry and is known for its strong pinning.[15–17] Recently, we have studied the details of the electronic structure, elastic properties, surface energies, and work functions of NiGe and PtGe.[12] We have reported that due to the almost covalent nature of bonding in these materials, Ni and Pt germanides exhibit unusual surface reconstructions, which await a detailed experimental study. Much less is known about the germanide-GaAs interface that is formed via rather complicated interfacial reactions.

In this paper, we study the interface between (001) oriented GaAs and the germanide alloy $Ni_{0.5}Pt_{0.5}Ge$. The composition of the germanide alloy is selected to minimize strain in the pseudoepitaxial film. By using density functional theory, we investigate the atomic and electronic structures of the interface and calculate the Schottky barrier height dependence on the GaAs(001) and NiPtGe(001) terminations. The rest of the paper is organized as follows: In Sec. II, we present the calculation methodology and atomic structure of the interface. In Sec. III, we discuss our calculations of the Schottky barrier height at the GaAs(001)/$Ni_{0.5}Pt_{0.5}Ge$(001) interface. In Sec. IV, we conclude with the details of the electronic structure of the interface and their relation to the electric properties.

II. CALCULATION METHODOLOGY AND INTERFACE MODEL

We use density functional theory[18] with the projected augmented wave[19] method, as implemented in the VASP code.[20] The Perdew–Burke–Ernzerhoff[21] form of the generalized gradient approximation for exchange and correlation is employed along with a standard plane wave basis set with a kinetic energy cutoff of 380 eV. The bulk calculations are performed with the $12\times12\times16$ Monkhorst–Pack[22] *k*-point mesh for the primitive orthorhombic cell. The supercell calculations that are used to estimate the Schottky barriers are done by using a $4\times4\times1$ mesh, which is found to be adequate in previous calculations.[12] The calculations are converged to 10^{-4} eV/cell and the structures are relaxed until the largest force becomes less than 0.05 eV/Å. This translates into better than 0.01 eV convergence in terms of the barrier estimate, which is based either on the density of states or on the average potential. We studied the issues that are related to the residual strain in the metallic layer, *k*-point sampling and energy cutoff in our previous papers.[12,23,24] The overall accuracy of the Schottky barrier estimate for a given geometry is on the order of 0.1 eV.

Both NiGe and PtGe crystallize in a primitive orthorhombic structure in the MnP- type lattice with space group *Pnma*

 ©2008 The American Physical Society

TABLE I. Theoretical and experimental lattice constants and internal in-plane coordinates of NiGe, PtGe, and $Ni_{0.5}Pt_{0.5}Ge$. The Ni (Pt) atoms are located at $[u_{Ni(Pt)}, v_{Ni(Pt)}, 1/4]$, $[(1/2-u_{Ni(Pt)}), (v_{Ni(Pt)}-1/2), 1/4]$, $[(1-u_{Ni(Pt)}), (1-v_{Ni(Pt)}), 3/4,]$, and $[(1/2+u_{Ni(Pt)}), (3/2-v_{Ni(Pt)}), 3/4]$, while the Ge atoms are located at $[u_{Ge}, v_{Ge}, 1/4]$, $[(3/2-u_{Ge}), (1/2+v_{Ge}), 1/4]$, $[(u_{Ge}-1/2), (1/2-v_{Ge}), 3/4]$, and $[(1-u_{Ge}), (1-v_{Ge}), 3/4]$.

Material		a (Å)	b (A)	c (A)	$u_{Ni(Pt)}$	$v_{Ni(Pt)}$	u_{Ge}	v_{Ge}
GaAs	Calc.	5.76						
	Expt.[a]	5.65						
NiGe	Calc.	5.84	5.36	3.50	0.1795	0.9933	0.577	0.1769
	Expt.[b]	5.79	5.37	3.43				
PtGe	Calc.	6.16	5.83	3.75	0.1922	0.9988	0.5884	0.1857
	Expt.[c]	6.09	5.72	3.70	0.1908	0.9995	0.5900	0.1850
$Ni_{0.5}Pt_{0.5}Ge$	Calc.	6.03	5.59	3.65	0.1708	0.9861	0.5987	0.1763
	Expt.							

[a]Reference 28
[b]Reference 29
[c]Reference 30.

(No. 62 in the international x-ray table).[12] The Ni (Pt) atoms are sixfold coordinated with Ge atoms. GaAs crystallizes in the zinc blende structure. The calculated lattice parameters of bulk NiGe, PtGe, $Ni_{0.5}Pt_{0.5}Ge$, and GaAs along with the experimental values are presented in Table I. A more detailed study of the electronic structure, elastic properties, surface energies, and work functions of PtGe and NiGe can be found in Ref. 12. We use theoretical minimum energy structures to build the interface model.

To simulate the interface, we use supercell geometry. Assuming GaAs to be the substrate for a NiGe film, the two calculated lateral in-plane lattice constants of NiGe (a and b) would have to be strained by −1.37% and 7.45%, respectively, to match the calculated bulk GaAs lattice constant. However, the strain can be reduced and balanced to only −4.48% and 3.04% by alloying Pt into NiGe and forming $Ni_{0.5}Pt_{0.5}Ge$. We have tried several compositions, but limited by the cell size, we have chosen the 50-50 alloy as the best. Our bulk $Ni_{0.5}Pt_{0.5}Ge$ unit cell contains two Ni, two Pt, and four Ge atoms with alternating planes of NiGe(001) and PtGe(001) along the c axis. Moving platinum atoms to other substitutional Ni sites changes the alloy lattice constants by only 0.01 Å or less. In addition to strain reduction, the alloying of NiGe and PtGe also allows for tuning of the work function of the alloyed metal film. As calculated in Ref. 12, the NiGe work function varies between 4.31 and 4.76 eV, while the PtGe work function varies between 4.58 and 5.01 eV, depending on the surface orientation. Our choice of the NiPtGe orientation is driven by its work function, relatively low surface energy,[12] reasonable interfacial structure, and by the cell-size limitations of the *ab initio* methods that are used here. We set the in-plane lattice constants of the semiconductor (GaAs) and the metal alloy (NiPtGe) films to bulk semiconductor lattice constant value. The resulting mixed compressive and tensile strain in the NiPtGe film is accommodated by elongation along the growth direction. The corresponding NiPtGe lattice constant c is calculated by minimizing the total energy of the appropriately strained NiPtGe unit cell. By using the average between the interplanar distances in the semiconductor and in the metal as a starting point, we optimize all internal degrees of freedom of the GaAs(001)/NiPtGe(001) supercell. The out of plain relaxation is important in a Schottky barrier calculation because it minimizes the effect of strain on the work function of the metal.

We would like to point out that there are several different levels of uncertainty in these types of calculations. First, they are still performed with relatively small cells, and choices are made in the analysis of the density of states and reference potential. For a given geometry, we estimate the overall accuracy of the calculation to be on the order of 0.1 eV. Second, there are issues with the theory itself. Interested readers may find a discussion of density functional theory's applicability to band discontinuity calculations in the paper of Godby and Sham.[25] The problems arise in the depletion region, where the band edge state is not occupied. In our case, the bulk quasiparticle correction in both materials is quite small,[26,27] and since our calculations are performed for the intrinsic semiconductor, the quasiparticle correction is expected to be small.

The supercell is composed of 17 alternating planes of Ga and As with 13 planes of $Ni_{0.5}Pt_{0.5}Ge(001)$ on top in a pseudoepitaxial arrangement, as shown in Fig. 1(a). Figures 2(a) and 2(b) show the (001) surface (1×1) unit cells of GaAs(001) and $Ni_{0.5}Pt_{0.5}Ge(001)$ surfaces. The entire simulation cell is shown in Fig. 2(c). The large thickness of the cell (almost 50 Å) is necessary for convergence of the site projected partial density of states (used in Sec. III for the analysis of the electronic structure) to bulk values away from the interface. The surface unit cell of NiPtGe (001) contains two metal (Ni or Pt) and two Ge atoms. The Ni atom at the NiPtGe(001) surface makes four bonds with neighboring surface and subsurface Ge atoms, while two Ge atoms are fourfold coordinated, which makes two bonds with neighboring Ni and two bonds with Pt atoms. Figure 1(a) shows the relaxed GaAs(001)/NiPtGe(001) interface for the case of As-terminated GaAs(001) and NiGe-terminated NiPtGe(001). At the relaxed interface, Ni atoms are fourfold and onefold co-

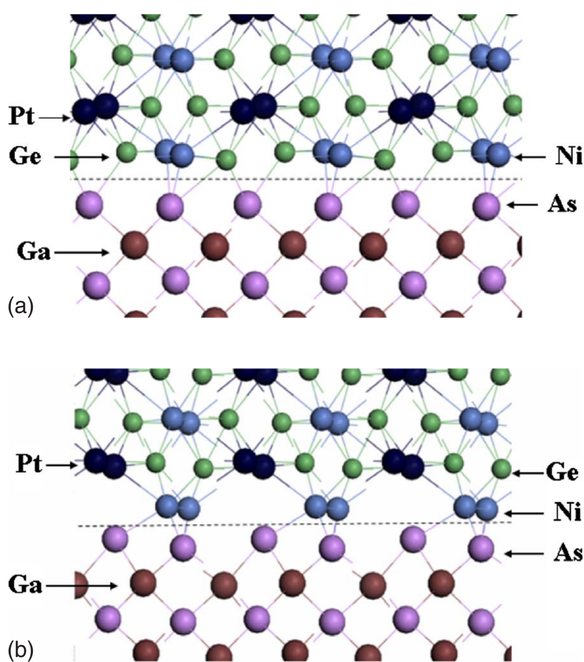

FIG. 1. (Color online) (a) Side view of GaAs(001)/NiPtGe(001) interface with As-terminated GaAs(001) and NiGe terminated NiPtGe (001) surface. The brown and violet balls are the Ga and As atoms, respectively, while the green, blue, and dark blue balls are the Ge, Ni, and Pt atoms, respectively. (b) Side view of GaAs(001)/NiPtGe(001) interface with As-terminated GaAs(001) and Ni terminated NiPtGe (001) surface with Ge vacancies. The brown and violet balls are the Ga and As atoms, respectively, while the green, blue, and dark blue balls are the Ge, Ni and Pt atoms, respectively.

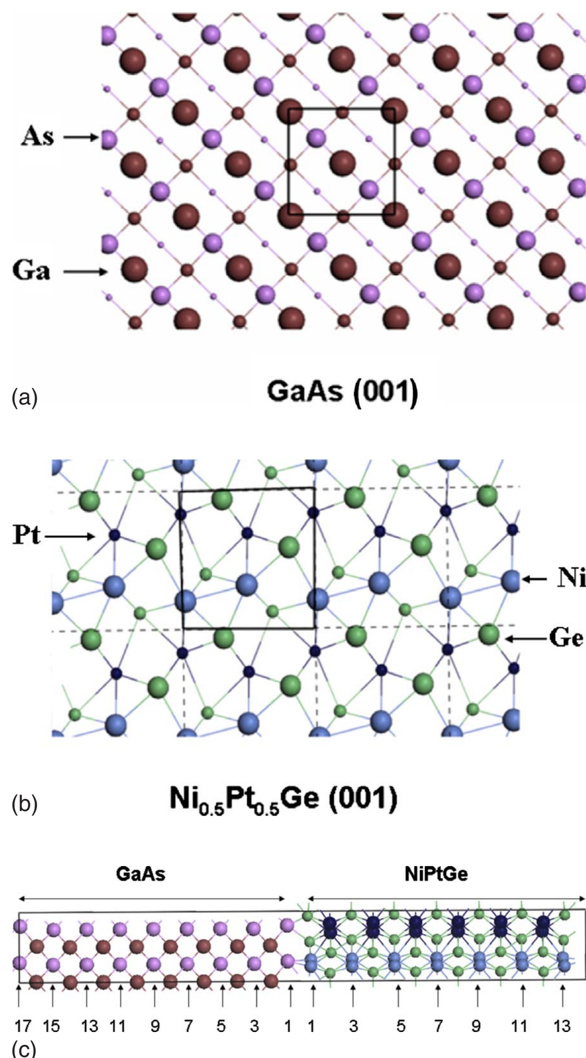

FIG. 2. (Color online) (a) Top view of GaAs(001) surface and surface unit cell. The brown and violet balls are the Ga and As atoms, respectively. (b) Top view of NiPtGe (001) surface and surface unit cell. The green, blue, and dark blue balls are the Ge, Ni, and Pt atoms respectively. The NiPtGe(001) surface unit cell contains two Ni (Pt) and two Ge atoms. (c) GaAs/NiPtGe supercell. The numbers indicate different layers in the GaAs and NiPtGe sides of the supercell. The brown and violet balls are the Ga and As atoms, respectively, while the green, blue, and dark blue balls are the Ge, Ni, and Pt atoms, respectively.

ordinated by Ge and As, respectively. There are two As atoms at the interface. The first one makes two bonds with Ga and two with Ni. The second is bonded to two Ga and two Ge atoms. Two Ge atoms at the interface make two bonds to Ni and two to Pt atoms, and one bond to As. The Ni-As bond length is 2.41 Å, which is close to the bond length between the nearest neighbor Ni and As atoms in bulk NiAs. Likewise, bond lengths between Ge and As are 2.50 and 2.65 Å. There are many possible ways to construct the GaAs/NiPtGe interface. We limit our study to considering interfaces of Ga- and As-terminated GaAs(001) with NiGe and PtGe terminated NiPtGe(001). We also consider two interfaces with Ge vacancies present.

III. SCHOTTKY BARRIER HEIGHT AT THE GaAs/NiPtGe INTERFACE

We first estimate the Schottky barrier height at the GaAs/NiPtGe interface by using semiempirical models. In a conventional Schottky model[31] (no Fermi level pinning), the *n*-type barrier height at the metal-semiconductor interface is given by the difference between the metal work function φ and electron affinity χ of the semiconductor (i.e., the energy difference between the conduction band edge and vacuum). Likewise, the *p*-type Schottky-barrier is the difference between the metal work function and the semiconductor valence band edge, $\chi+E_g-\varphi_m$. The calculated values of the work function of NiGe-terminated and PtGe-terminated $Ni_{0.5}Pt_{0.5}Ge(001)$ surfaces are 4.52 and 4.80 eV, respectively. It is interesting to note that these values are very close to the NiGe(001) and PtGe(001) work functions of 4.57 and 4.83 eV.[12] With $\chi+E_g=5.50$ eV for GaAs(001),[32] the *p*-type barrier at the GaAs(001)/NiPtGe(001) interfaces would be 0.98 and 0.70 eV in the Schottky limit for these two terminations of the NiPtGe(001). In the Schottky limit, the *p*-SBH changes with the metal work function in a linear fashion. Reference 12 lists the NiGe and PtGe work functions as a function of surface termination. For instance, the NiGe work function varies between 4.31 and 4.76 eV, while the PtGe work function varies between 4.58 and 5.01 eV. Thus, in the Schottky limit, the *p*-SBH at the GaAs-NiPtGe interface can

vary by a few tenths of a volt, depending on the work function of the NiPtGe surface. Alternatively, in the Bardeen limit (strong pinning),[33] the p-type barrier is the difference between the charge neutrality level (ϕ_{CNL}) and the top of the semiconductor valence band. The charge neutrality level in GaAs is 0.70 eV above the valence band edge.[34] Thus, in the Bardeen limit, the p-type barrier would be 0.70 eV, which is independent of the metal work function. However, experimentally, p-SBH at metal-GaAs interfaces is found to lie between 0.4 and 0.6 eV, which weakly depends on the metal work function.[4] Perhaps a more reasonable estimate of the p-SBH can be inferred from the metal induced gap states (MIGSs) model[35] that linearly interpolates between the Bardeen and the Schottky limits. The MIGS p-type barrier ϕ_p is given by

$$\phi_p = E_g - S(\phi_m - \phi_{\text{CNL}}) - (\phi_{\text{CNL}} - \chi).$$

Here, ϕ_{CNL} is the charge neutrality level that is measured from the vacuum level, E_g is the valence band gap of the semiconductor, and ϕ_m is the work function of the metal. S is the empirical pinning parameter that describes the screening by the interfacial states,[36]

$$S = \frac{1}{1 + 0.1(\varepsilon_\infty - 1)^2},$$

where ε_∞ is the high frequency limit of the dielectric constant of the semiconductor. For $S=0$ and 1, one regains the Bardeen and the Schottky limits, respectively. Taking ε_∞ equal to 10.7 for GaAs,[32] the S factor is 0.096 (strong pinning). By using a value of 4.07 eV for the GaAs electron affinity, we estimate the p-type barrier to be 0.71 eV, which is close to the Bardeen limit. This is expected since the Fermi level at the GaAs surface is strongly pinned (as described by the pinning factor S). The MIGS estimate of the p-SBH very weakly depends on the work function of the metal because of the very small value of the pinning factor S. For instance, a variation of 0.5 eV in the metal work function would change the MIGS estimate of p-SBH by less than 0.05 eV. We must note that there are number of limitations with the MIGS and other empirical models, as described in detail in Ref. 37. Generally, semiempirical models are unable to describe the dependence of the SBH on the interface structure. On the other hand, *ab initio* calculations properly take into account the interface bonding and, thus, properly capture the dependence of the SBH on the interface atomic structure.

We perform first principles calculations of the Schottky barrier by using a supercell, as described in Sec. II. To calculate the Schottky barrier height, we need to know the Fermi level and the GaAs valence band edge positions. We follow the procedure that was originally introduced by Bylander and Kleinman[38] with the exception that only the average electrostatic potential is calculated across the supercell, as suggested by Van de Walle and Martin.[39] We first compute the planar average of the electrostatic potential and then its macroscopic average $\bar{V}_{\text{GaAs}}$ in the region away from the interface that we believe to be bulklike. Placing the valence band edge with respect to the macroscopic average potential requires a separate calculation for bulk GaAs, wherein we

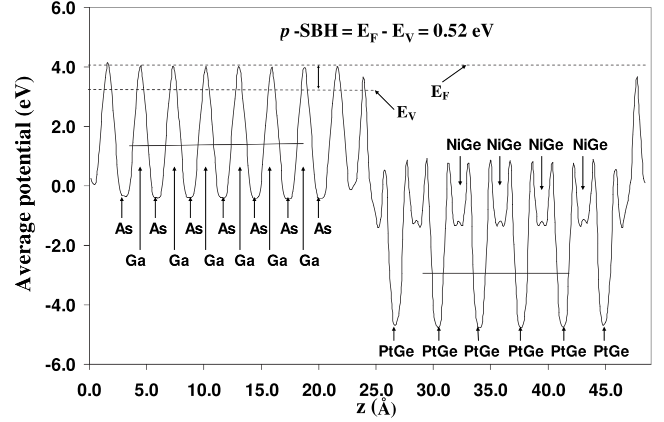

FIG. 3. The average Coulomb potential (in eV) in the GaAs(001) and NiPtGe portions of the supercell along z (growth axis). The GaAs(001) is As-terminated and NiPtGe(001) is NiGe terminated.

find the valence band maximum to be $E_{\text{VBM}}=2.06$ eV above the reference $\bar{V}_{\text{GaAs}}$. In the case of a GaAs(001)/NiPtGe(001) supercell with As-terminated GaAs(001) and Ni-Ge terminated NiPtGe(001), the average electrostatic potential and Fermi energies are at 4.01 and 1.43 eV, respectively (see Fig. 3). By using the bulk reference to locate the valence band top, we calculate the barrier height of 0.52 eV from

$$\phi_p = E_F - (\bar{V}_{\text{Si}} + E_{\text{VBM}}).$$

We calculate p-SBH at GaAs/NiPtGe interfaces with different GaAs(001) and NiPtGe(001) terminations and Ge vacancies. The calculated values of the p-SBH are listed in Table II. It can be seen that the p-SBH varies by as much as 0.18 eV and is within the experimental range.[4] Looking more carefully, we notice that interfaces involving As-Ge bonding result in similar barriers. The p-SBH variation is least when Ge and As atoms are bonded at the interface. The calculated p-SBH is 0.52 eV when GaAs(001) is As terminated and NiPtGe(001) is NiGe or PtGe terminated. For the interfaces that are free of As-Ge bonds, the pinning is not so strong. To further clarify this interesting observation, we need to take a closer look at the electronic structure of the interface.

TABLE II. Calculated p-Schottky barrier heights at the GaAs/NiPtGe interface with different GaAs(001) and NiPtGe(001) termination.

Interface	GaAs(001)	NiPtGe(001)	p-SBH (eV)
GaAs/NiPtGe	As terminated	Ni-Ge terminated	0.52
GaAs/NiPtGe	As terminated	Ni terminated (Ge vacancies)	0.46
GaAs/NiPtGe	Ga terminated	Ni-Ge terminated	0.47
GaAs/NiPtGe	Ga terminated	Ni terminated (Ge vacancies)	0.64
GaAs/NiPtGe	As terminated	Pt-Ge terminated	0.52
GaAs/NiPtGe	Ga terminated	Pt-Ge terminated	0.59

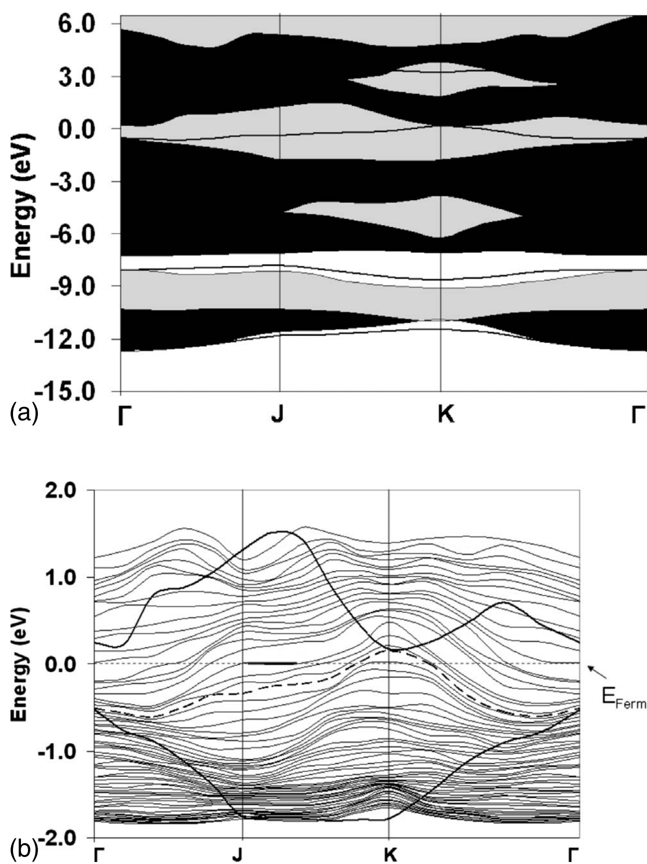

FIG. 4. (a) Two-dimensional band structure for GaAs/NiPtGe interface [GaAs(001) is As-terminated and NiPtGe is NiGe terminated]. Bulk band structure of GaAs (dark area) and NiPtGe (gray and dark areas) that is projected along [001] is also shown. Some interface bands are shown by the dark lines. The Fermi energy is at 0 eV. (b) Two-dimensional band structure of GaAs/NiPtGe in the region of the semiconductor band gap. The dark lines are boundaries of GaAs band structure projected along [001]. The short solid line marks the occupied states responsible for the Fermi level pinning. The dashed line is the resonance state whose charge density is shown in Fig. 6(a) [GaAs(001) is As terminated and NiPtGe is NiGe terminated]. The complete band structure is shown in Fig. 4(a).

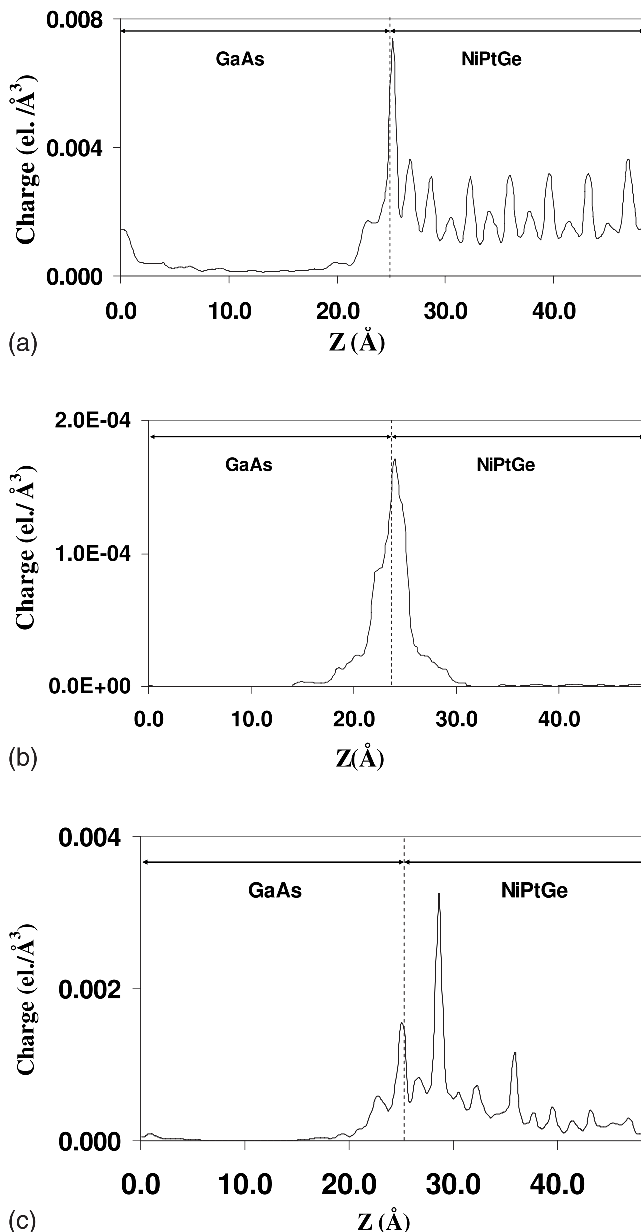

FIG. 5. (a) Charge density (planar average) along the slab axis for the dashed band, as shown in Fig. 4(b). The vertical dotted line indicates the interface position that is defined to be halfway between As and Ge atoms. (b). Charge density along the slab axis for the band, as shown in the Fig. 4(a), around 8 eV. The vertical dotted line indicates the interface position. (c) Charge density along the slab axis for the band segment crossing the Fermi level [the short solid line in Fig. 4(b)]. The vertical dotted line indicates the interface position.

IV. ELECTRONIC STRUCTURE OF THE GaAs(001)/ NiPtAs(001) INTERFACE

Figure 4(a) projects the bulk band structures of GaAs (dark area) and NiPtGe (gray area) into the GaAs/PtNiGe interfacial plane. The Fermi level is at zero energy. Figure 4(a) indicates that localized interface bands occur deep in the valence band of the semiconductor around 8 and 12 eV below the Fermi level. The interface state in the mutual band gap at around -8 eV is mainly formed by Ge *p* orbitals, while the state at around -12 eV is from As *s* orbitals. Several metal induced gap states, i.e., interface resonances, are present in the GaAs gaps, of which two of the most prominent are indicated by the bold lines, as are the localized interface bands. Figure 4(b) shows all of the calculated NiPtGe bands in the semiconductor energy gap, many but not all of which are resonances. In Fig. 5(a), we show the charge density of the band that is indicated by the dotted line in Fig. 4(b). Note that the wave functions rapidly decay into the semiconductor but are sustained on the metal side. Localized interface states can exist in the mutual gaps of the projected band structure of two bulk materials. In Fig. 5(b), we show the charge density that corresponds to the band around 8 eV in Fig. 4(a), which is in a mutual gap.

Figure 6(a) shows the partial density of states (PDOS) that are projected onto the *p* states of As atoms that are

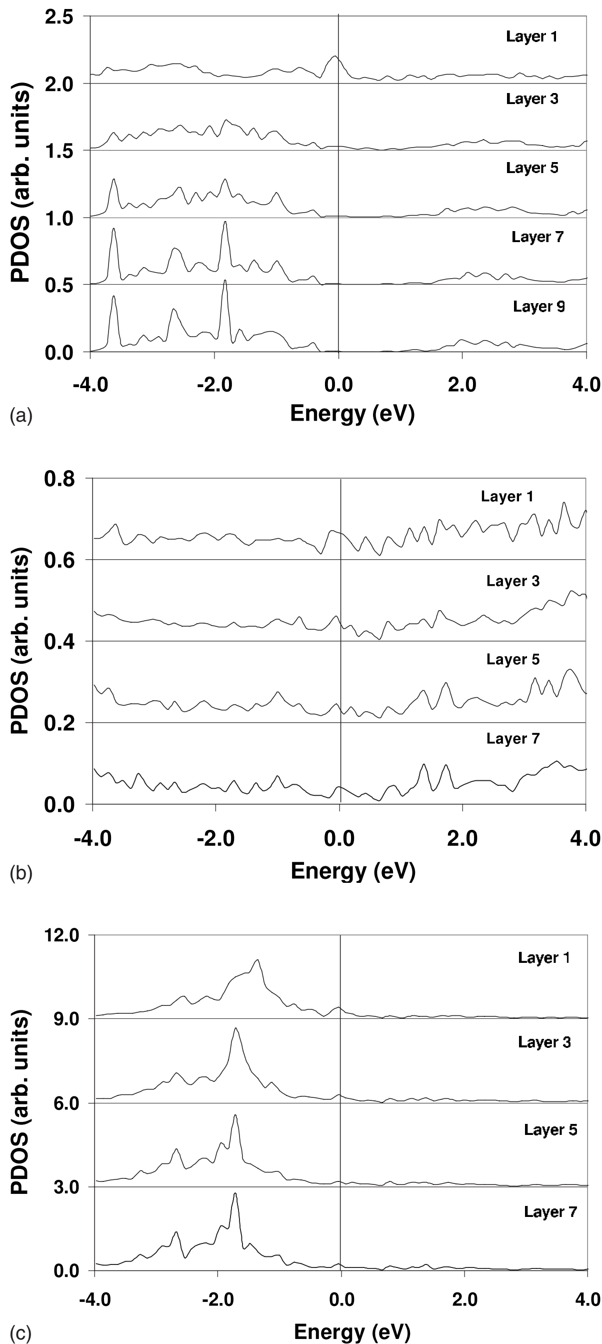

FIG. 6. (a) Density of states projected on p orbitals of As atom that is located in different layers [Fig. 2(c)] from the NiPtGe/GaAs interface in the supercell [GaAs(001) is As terminated and NiPtGe is NiGe terminated]. The topmost DOS denotes the nearest from the interface, while the bottom-most denotes farthest from the interface. (b) Density of states projected on p orbitals of Ge atom that is located in different layers [Fig. 2(c)] from the NiPtGe/GaAs interface in the supercell [GaAs(001) is As terminated and NiPtGe is NiGe terminated]. The topmost DOS denotes the nearest from the interface, while the bottom-most denotes the farthest from the interface. (c) Density of states projected on d orbital of Ni atom that is located in different layers [Fig. 2(c)] from the NiPtGe/GaAs interface in the supercell [GaAs(001) is As-terminated and NiPtGe is NiGe terminated]. The topmost DOS denotes the nearest from the interface, while the bottom-most denotes farthest from the interface.

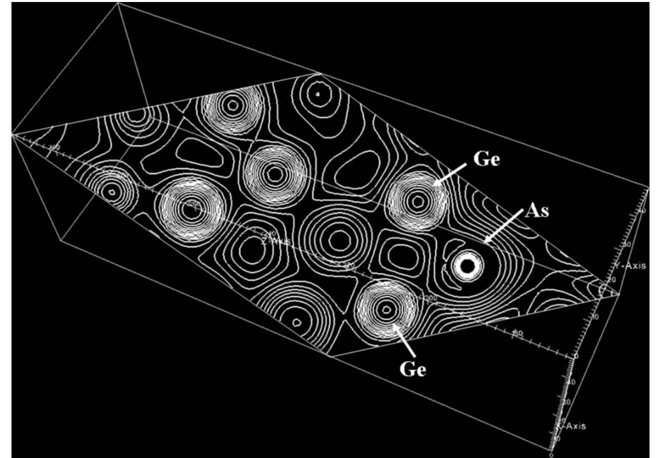

FIG. 7. The contour plot showing the Ge-As bond at the interface for band segment crossing the Fermi level [the short solid line in Fig. 4(b)].

located in different layers in the GaAs side of the As-terminated GaAs(001) and NiGe-terminated NiPtGe(001) interface. The PDOS at the interface significantly differs from that in the bulk. In particular, we notice a large peak at the Fermi level, which rapidly decays inside the semiconductor. Figures 6(b) and 6(c) show the density of states that are projected on the Ge atoms (p states) and Ni atoms (d states) that are located in different layers of NiPtGe and GaAs, respectively. Ge atoms produce a peak at the Fermi level. The peak does not completely decay but diminishes by a factor of 2 as we move away from the interface since it is a resonance with respect to the metal's band structure. We also see a peak at the Fermi level in the Ni-projected states. The d-orbital projected DOS regains its bulk structure five layers into the metal.

The interface resonances in the GaAs band gap are formed mainly by As and Ge p orbitals and Ni d orbitals. In Fig. 7, we show a contour plot through the interface plane of the charge density that corresponds to the partially occupied flatband near the Fermi level, as shown in Fig. 4(b). The distribution strongly resembles a covalent bond. The distribution of charge in this band in the direction normal to the interface is shown in Fig. 5(c); the distribution is characterized by two main peaks: one at the interface and one at approximately 3 Å inside the germanide. This band corresponds to the PDOS peaks that come from the interfacial Ge and As, as we see in Figs. 6(a) and 6(b). Looking at Table II, we thus propose that As-Ge bonds at the GaAs/NiPtGe interface may cause the Fermi level pinning. Although the statement is tentative, it is clear that the barrier shows some variation for all other interfaces, and even for this one if As-Ge bonding is interrupted, e.g., with Ge vacancies. The p-SBH varies by as much as 0.18 eV around the pinned value of 0.52 eV.

V. CONCLUSION

We have studied the atomic and electronic structures of the GaAs(001)/NiPtGe(001) interface with different

GaAs(001) and $NiPtGe_2$(001) terminations using density functional theory. The calculated *p*-Schottky barrier values vary by as much as 0.18 eV around the average value of 0.52 eV, which corresponds to the pinned interface. Through a detailed analysis of the electronic structure of the interface, we find that the interfacial Ge-As bonds result in a high density of states at the Fermi level. We suggest this to be a microscopic origin of the Fermi level pinning at the GaAs/NiPtGe interface. These findings will be useful in the future process development.

ACKNOWLEDGMENTS

We thank Prashant Majhi for discussions and sharing experimental results with us prior to publication. We are grateful to Conal Murray, Stefan Zollner, Mehmet Öztürk, and Jaekwang Lee for insightful discussions. This work was supported by the Semiconductor Research Corporation under Contract No. 2006-JV-1439, by the Welch Foundation under Grant No. F-0934, and by the Texas Advanced Computing Center.

*demkov@physics.utexas.edu

[1] S. Datta, T. Ashley, J. Brask, L. Buckle, M. Doczy, M. Emeny, D. Hayes, K. Hilton, R. Jefferies, T. Martin, T. Philips, D. Wallis, P. Wilding, and R. Chau, Tech. Dig. - Int. Electron Devices Meet. **2005**, 34.1.
[2] S. Datta, Microelectron. Eng. **84**, 2133 (2007).
[3] R. Droopad, K. Rajagopalan, J. Abrokwah, P. Zurcher, and M. Passlack, Microelectron. Eng. **84**, 2138 (2007).
[4] M. Murakami and Y. Koide, Crit. Rev. Solid State Mater. Sci. **23**, 1 (1998).
[5] S. Zhang and M. Ostling, Crit. Rev. Solid State Mater. Sci. **28**, 1 (2003).
[6] C. H. Huang, D. S. Yu, Albert Chin, C. H. Wu, W. J. Chen, Chunxiang Zhu, M. F. Li, Byung Jin Cho, and Dim-Lee Kwong, Tech. Dig. - Int. Electron Devices Meet. **2003**, 13.4.1.
[7] Shiyang Zhu, L. Rui, S. J. Lee, M. F. Li, A. Du, J. Singh, C. Zhu, A. Chin, and D. L. Kwong, IEEE Electron Device Lett. **26**, 81 (2005).
[8] D. Z. Chi, R. T. P. Lee, S. J. Chua, S. J. Lee, S. Ashok, and D.-L. Kwong, J. Appl. Phys. **97**, 113706 (2005).
[9] R. Nath, C. W. Woo, C. B. Boothroyd, M. Yeadon, D. Z. Chi, H. P. Sun, Y. B. Chen, X. Q. Pan, and Y. L. Foo, Appl. Phys. Lett. **86**, 201908 (2005).
[10] B. Balakrisnan, C. C. Tan, S. L. Liew, P. C. Lim, G. K. L. Goh, Y. L. Foo, and D. J. Chi, Appl. Phys. Lett. **87**, 241922 (2005).
[11] F. Nemouchi, D. Mangelinck, C. Bergman, G. Clugnet, P. Gas, and J. L. Labar, Appl. Phys. Lett. **89**, 131920 (2006).
[12] M. K. Niranjan, L. Kleinman, and A. A. Demkov, Phys. Rev. B **75**, 085326 (2007).
[13] G. Y. Robinson, in *Physics and Chemistry of III-V Compound Semiconductor Interfaces*, edited by C. W. Wilmsen (Plenum, New York, 1985), p. 195.
[14] S. M. Sze, *Physics of Semiconductor Devices* (Wiley, New York, 1981), p. 245.
[15] R. G. Dandrea and C. B. Duke, J. Vac. Sci. Technol. A **11**, 848 (1993).
[16] R. G. Dandrea and C. B. Duke, J. Vac. Sci. Technol. B **11**, 1553 (1993).
[17] C. Berthod, N. Binggeli, and A. Baldereschi, Phys. Rev. B **68**, 085323 (2003).
[18] W. Kohn and L. J. Sham, Phys. Rev. **140**, A1133 (1965).
[19] P. E. Blöchl, Phys. Rev. B **50**, 17953 (1994).
[20] G. Kresse and J. Furthmuller, Phys. Rev. B **54**, 11169 (1996).
[21] J. P. Perdew, K. Burke, and M. Ernzerhof, Phys. Rev. Lett. **77**, 3865 (1996).
[22] H. J. Monkhorst and J. D. Pack, Phys. Rev. B **13**, 5188 (1976).
[23] M. K. Niranjan, S. Zollner, L. Kleinman, and A. A. Demkov, Phys. Rev. B **73**, 195332 (2006).
[24] M. Niranjan, L. Kleinman, and A. A. Demkov, *Advance Intermetallic-Based Alloys*, MRS Symposia Proceedings No. 980 (Materials Research Society, Warrendale, PA, 2007), Paper No. 0980-II05-43.
[25] R. W. Godby and L. J. Sham, Phys. Rev. B **49**, 1849 (1994).
[26] S. B. Zhang, M. L. Cohen, S. G. Louie, D. Tomanek, and M. S. Hybertsen, Phys. Rev. B **41**, 10058 (1990).
[27] F. Aryasetiawan, Phys. Rev. B **46**, 13051 (1992).
[28] C. Kittel, *Introduction to Solid State Physics*, 6th ed. (Wiley, New York, 1986).
[29] J. Y. Spann, R. A. Anderson, T. J. Thornton, G. Harris, and C. Tracy, IEEE Electron Device Lett. **26**, 151 (2005).
[30] E. J. Graeber, R. J. Baughman, and B. Morosin, Acta Crystallogr. B **29**, 1991 (1973).
[31] W. Schottky, Z. Phys. **113**, 367 (1939).
[32] S. Adachi, *Properties of Group-IV, III-V, and II-VI Semiconductors* (Wiley, Chichester, West Sussex, UK, 2005).
[33] J. Bardeen, Phys. Rev. **71**, 717 (1947).
[34] F. Flores, A. Munoz, and J. C. Duran, Appl. Surf. Sci. **41-42**, 144 (1989).
[35] V. Heine, Phys. Rev. **138**, A1689 (1965).
[36] J. Robertson and C. W. Chen, Appl. Phys. Lett. **74**, 1168 (1999).
[37] R. T. Tung, Phys. Rev. Lett. **84**, 6078 (2000).
[38] D. M. Bylander and Leonard Kleinman, Phys. Rev. B, **36**, 3229 (1987).
[39] C. G. Van de Walle and R. M. Martin, Phys. Rev. B **34**, 5621 (1986).